JOURNAL OF SOLID STATE CHEMISTRY 90, 8–16 (1991)

The Question of Silver Pairing in the New Structurally Resolved Two-Dimensional Phase $Ag_2MnP_2S_6$

M. EVAIN, F. BOUCHER, AND R. BREC

I.P.C.M., Laboratoire de Chimie des Solides, 2 rue de la Houssinière, 44072 Nantes Cédex 03, France

AND Y. MATHEY

Groupe de Physique des Etats Condensés, Université d'Aix Marseille 2, U.A. 783 Luminy, Case 901, 13288 Marseille Cédex 02, France

Received March 12, 1990; in revised form May 24, 1990

$Ag_2MnP_2S_6$ has been obtained as single crystals by solid state reaction from the elements in the atomic ratio Ag/Mn/P/S = 2/1/2/6. It crystallizes in the monoclinic system, nonconventional space group $C2/n$, a = 634.75(6) pm, b = 1095.2(1) pm, c = 1391.42(13) pm, β = 108.260(9)°, and Z = 4. The structure was refined in a split model by a least-squares method to a final R value of 0.033 from single-crystal diffractometer data with 995 independent structure factors. The Ag atoms are distributed on three different sites, the preponderate one being triangularly coordinated. Omitting the strong distortion induced at the silver sites, P_2S_6 and MnS_6 groups were found to be similar to that of $Mn_2P_2S_6$. From interatomic distance considerations (d_{Ag-Ag} =338 pm), silver–silver homobond could be ruled out.

I. Introduction

The interaction of d^{10} cations within cluster-like aggregates through short homoatomic contacts is well documented (*1*) and seems to take place specifically for d^{10} cation-rich compounds. Even if the origin of such interactions are not yet perfectly understood and if certain homoatomic links have not always been formally established, their occurrence cannot be denied. These interactions affect both the structure and the physical properties (*2, 3*) and can take place in many coordination types, from linear configuration to large irregular geometry, provided that they favor a mutual d^{10} cation proximity. Several authors have underlined the presence of partial s or s and p character in the d functions, that is, the formation of hybridized valence orbitals (*4–6*). Isolated d^{10} cations also present particular behaviors: High symmetry coordinations (octahedral and tetrahedral for instance) are usually unstable and distort to lower symmetry geometries that allow a mixing of filled and unfilled orbitals of similar energy (*7*).

The $M_2P_2S_6$ family (commonly referred to as MPS_3 phases) and its derivatives present different cases of d^{10} cations with particular characteristics. For instance, in $Cd_2P_2S_6$ and $Zn_2P_2S_6$ (*8*), the closed shell cations exhibit large thermal parameters (B_{eq}). According to a recent infrared (IR) study and a

0022-4596/91 $3.00

valence force field calculation (*9*), it has been shown that the high B_{eq} of Zn^{2+} or Cd^{2+} cations (isoelectronic with Ag^+) does not correspond to strong vibrations, but to a shift from the octahedral center to off-center positions, identical for each (MS_6) group, but differing in their orientations from site to site. The same phenomenon is found in $AgMP_2S_6$ (M = Cr, V) (*10*) and $AgVP_2Se_6$ (*11*) where Ag^+ seems to be randomly distributed on different positions (possibly six) shifted with respect to the octahedron center toward its triangular windows. Copper is also known to present particular behavior in $CuMP_2S_6$ phases (M = Cr, V) (*12*). In $CuVP_2S_6$, for instance, three different identifiable sites were found, one near the center of the M^1 octahedron, another one close to the triangular face of this octahedron, and the last one in a van der Waals tetrahedral position. Again in that case, and maybe for reasons similar to those underlined above, none of these copper atoms sit in the very center of the anionic polyhedra. Beyond the rather worthwhile systematic feature of the isolated d^{10} cations, the possible occurrence of bonded copper pairs in the copper substituted phases of the (2D) $M_2P_2S_6$ type is still an open question. In opposition, a closeness of two silver cations can be envisioned in $Ag_2MnP_2S_6$ in which two Ag(I) ions must share, in the hypothesis of a classical $M_2P_2S_6$ layered arrangement, the same octahedron. EXAFS studies on one hand (*13*) and IR and Raman spectroscopies on the other hand (*14*) suggested possible arrangements and localizations for Ag(I) and hinted to a possible Ag(I)–Ag(I) grouping.

To help bring up more information on this phase within the scope of Ag(I) behavior in chalcogenides, we report, in this paper, the structure determination of $Ag_2MnP_2S_6$ and discuss, from the split model description of the phase, the question of silver pairing.

II. Experimental

Synthesis and analysis. Small apple green plates, suitable for crystallographic investigation, were obtained by heating of stoichiometric proportions of pure elemental silver, manganese, phosphorus, and sulfur at 560°C for 30 days in an evacuated silica tube. Their analysis by means of a SEM apparatus confirmed the 2 : 1 : 2 : 6 ratio of the title formulation. To ascertain the homogeneity of the phase for powder data indexation and magnetic susceptibility recording purposes (vide infra), another synthesis was made with the above exposed procedure followed by a room temperature grinding and a 2-week sintering at 350°C. Previous high temperature preparations (≈700°C) had led to a mixture in which one could distinguish, in a SEM observation, $Mn_2P_2S_6$, $Ag_2MnP_2S_6$, and $Ag_4P_2S_7$ phases, and various crystals with compositions in between that of $Ag_2MnP_2S_6$ and that of an hypothetical $AgMn_2P_2S_6$.

X-ray powder data. The cell parameters, initially estimated from Bragg and Weissenberg photographs (vide infra), were least-squares refined from INEL diffractometer data (CPS120 curve detector, $CuK_{\alpha 1}$ = 154.06 pm, and Ge as standard) using the first 60 lines (Table I). A first glance at these parameters (a = 634.75(6) pm, b = 1095.2(1) pm, c = 1391.42(13) pm, β = 108.260(9)°, and V = 918.5(2) × 10^6 pm^3) reveals an important expansion of the cell with respect to that of $Mn_2P_2S_6$ (a = 607.7(1) pm, b = 1052.4(3) pm, 2^*c = 1359.2(2) pm, b = 107.35(2), and 2^*V = 829.4(10) × 10^6 pm^3) (*8a*).

Single crystal studies. Although the finding of a proper single crystal proved difficult, on account of heavy twinning, a small flat adequate crystal (0.31 × 0.22 × 0.008 mm^3) was sorted out. Classical film analysis yielded a C-centered monoclinic cell, space group $C2/c$ and $\beta \approx 98°$. In order to ease comparisons with previous $M_2P_2S_6$ phases,

TABLE I

X-RAY POWDER DIFFRACTION OF $Ag_2MnP_2S_6$

d_{obsd} (pm)	d_{calcd} (pm)	$h\ k\ l$	I_{calcd}[a]
544.4	544.6	1 1 −1	45.9
505.0	505.9	0 2 1	14.8
395.6	395.9	1 1 −3	20.7
343.2	343.2	0 2 3	36.5
330.2	330.3	0 0 4	92.7
314.0	313.9	2 0 −2	50.5
312.5	312.3	1 3 0	100.0
300.4	300.1	1 1 3	31.5
274.0	273.8	2 2 −1	36.3
272.5	272.3	2 2 −2	6.0
267.9	268.1	0 4 1	10.6
266.2	266.1	1 3 2	13.5
248.1	247.9	1 3 −4	6.9
246.6	246.6 246.3	2 0 2 2 2 1	11.2
238.0	238.0	0 2 5	6.0
232.6	232.5	0 4 3	23.0
226.6	226.6	1 1 −6	1.9
224.9	224.8	2 2 2	2.0
219.3	219.3	2 2 −5	30.9
212.4	212.3	2 0 −6	3.5
210.6	210.5	1 3 4	6.9
206.8	207.0 206.8	2 4 −1 1 5 −1	8.9
206.2	206.3	2 4 −2	2.3
204.9	204.9	3 1 −1	4.4
204.3	204.3	0 2 6	3.8
203.2	203.2	2 2 3	19.9
202.7	202.8	1 5 −2	0.8
198.94	198.71	3 1 4	1.2
195.56	195.54	1 3 −6	3.3
194.34	194.28	2 4 1	5.7
190.18	190.14	0 4 5	7.2
188.59	188.58	3 1 −5	9.4
187.20	187.20	3 1 1	2.5
185.92	185.93	1 1 6	3.1
183.02	183.05	3 3 −2	38.0
182.52	182.53	0 6 0	18.7
180.20	180.19	2 4 −5	5.7
179.32	179.28	1 5 3	7.7

[a] Intensities calculated with the Lazy Pulverix program (*13*) for a Debye Scherrer geometry and with anomalous dispersion.

a transformation to the above-mentioned cell was performed, leading to the unconventional space group $C2/n$. Data collection was carried out at room temperature on a CAD4-Kappa diffractometer (Enraf–Nonius) with standard recording conditions (see Table II). Omitting systemic nul reflections due to C centering, a total of 4417 data were recorded in the $-h/h$, $0/k$, and $-l/l$ space portion. After usual data reduction, including Lorentz polarization and absorption correction (μ = 70.6 cm^{-1}), a set of 994 independent reflections with $I > 3\sigma(I)$ was available for structure refinements.

III. Structure Refinement

Structural least-squares refinements were accomplished with the SDP-PLUS software package (1982 version) distributed by Enraf–Nonius (*15*). Looking for the well-known $M_2P_2S_6$ sulfur packing octahedrally enclosing P_2 pairs and M^{II} cations and seeking Ag cations in triangular environment, the Patterson map was easily unraveled. With isotropic thermal factors and the whole set of atomic positions, but extra silver ones (vide infra), the reliability factor converged to the rather high value R = 27.4%. The introduction of the anisotropy thermal motion for all the atoms strikingly lowered that value to 4.1%. At this stage of the calculation, Fourier and Fourier difference maps showed two unaccounted for maxima on both sides of the already included silver atom. The introduction of those two residues with appropriate partial occupation ratios led to the new reliability factor R = 3.3%, significantly demarked from the previous result. A new Fourier difference map calculation did not exhibit meaningful features. Fractional coordinates and thermal parameters of the eight independent atoms of the cell are gathered in Tables III and IV, respectively.[1]

[1] See NAPS document No. 04821 for 11 pages of supplementary material. Order from ASIS/NAPS. Microfiche Publications, P.O. Box 3513, Grand Central Station, New York, NY 10163. Remit in advance $4.00 for microfiche copy or for photocopy, $7.75 up to 20 pages plus $.30 for each additional page. All orders

TABLE II

ANALYTICAL AND CRYSTALLOGRAPHIC DATA: PARAMETERS OF THE X-RAY DATA COLLECTION AND REFINEMENT

1. Physical, crystallographic, and analytical data			
Formula	$Ag_2MnP_2S_6$	Molecular weight	524.98 g/mole^{-1}
Space group	$C2/n$ (15)		
Room temperature crystallographic constants			
	a = 634.75(6) pm	β = 108.260(9)°	
	b = 1095.2(1) pm	z = 4	
	c = 1391.42(13) pm		
Density (calcd)	3.787		
Absorption factor	μ(Mo$K\alpha$) = 70.6 cm^{-1}		
Crystal size	0.31 × 0.22 × 0.008 mm^3		
2. Data collection			
Temperature	273 K		
Radiation	Mo$K\alpha$	Monochromator	Oriented graphite (002)
Scan mode	$\omega/2\theta$	Scan angle	1.5 + 0.35 tan (θ)
Recording range	1.5–35°		
Standard reflections	2 −6 0, −1 −3 1, −2 8 −3 (every 3600 sec)		
3. Refinement conditions			
Reflections for crystal matrix orientation			25
Recorded reflections in a $\frac{1}{2}$ space			4417
Independent reflections with $I > 3\sigma(I)$ and $\sin(\theta)/\lambda < 0.75$			994
Refined parameter			73
Reliability factors		$R = \Sigma\|F_o\| - \|F_c\|/\Sigma\|F_o\|$	
		$R_w = (\Sigma(\|F_o\| - \|F_c\|)^2/\Sigma F_o^2)^{1/2}$	
Weighting scheme	Unit weights		
4. Refinement results			
R = 3.3%	R_w = 3.6%		
Extinction coefficient	$E_c = 5.0(1) \times 10^{-7}$		
Difference Fourier maximum peak intensity	0.8(2) × 10$^{-6}e^-$/pm^3		

IV. General Structural Pattern

Although the $Ag_2MnP_2S_6$ structural arrangement is closely related to that of the $M_2P_2S_6$ phases, it belongs to a new variety: the $M^I_2M^{II}P_2S_6$ type. Indeed, like all the $M_2P_2S_6$ structures, the $Ag_2MnP_2S_6$ structure

TABLE III

POSITIONAL PARAMETERS AND THEIR ESTIMATED STANDARD DEVIATION

Atom	x	y	z	B_{eq}[a] (×10^{-4})	τ
Ag1	0.6695(1)	0.41263(7)	0.12210(8)	4.43(2)	0.812(2)
Ag2	0.6318(7)	0.4109(5)	0.0869(3)	2.87(8)	0.134(2)
Ag3	0.727(1)	0.410(1)	0.169(1)	5.3(2)	0.077(2)
Mn	0.25	0.5778(1)	0.25	1.24(2)	
P	0.6961(2)	0.7530(1)	0.66547(9)	0.80(2)	
S1	0.5566(2)	0.5877(1)	0.6195(1)	1.12(2)	
S2	0.4719(2)	0.6087(1)	0.1194(1)	1.13(2)	
S3	0.5287(2)	0.7188(1)	0.3763(1)	1.15(2)	

[a] Isotropic equivalent thermal parameter defined as $B_{eq}(pm^2) = \frac{1}{3}\Sigma_i \Sigma_j \beta_{ij} a_i a_j$.

must be prepaid. Institutions and Organizations may order by purchase order. However, there is a billing and handling charge for this service of $15. Foreign orders add $4.50 for postage and handling, for the first 20 pages, and $1.00 for additional 10 pages of material, $1.50 for postage of any microfiche orders.

TABLE IV
THERMAL PARAMETERS: Us ($\times 10^{-4}$ pm^2)

Atom	U_{11}	U_{22}	U_{33}	U_{12}	U_{13}	U_{23}
Ag1	0.0262(2)	0.0160(2)	0.1369(6)	0.0006(3)	0.0411(3)	0.0028(4)
Ag2	0.031(1)	0.035(2)	0.047(2)	−0.003(2)	0.018(1)	−0.001(2)
Ag3	0.027(3)	0.061(5)	0.113(8)	0.011(4)	0.024(4)	0.004(7)
Mn	0.0189(4)	0.0128(4)	0.0184(5)	0	0.0104(3)	0
P	0.0129(4)	0.0087(4)	0.0122(4)	−0.0002(4)	0.0090(3)	0.0003(5)
S1	0.0161(4)	0.0099(4)	0.0183(5)	−0.0014(5)	0.0078(4)	−0.0012(5)
S2	0.0167(4)	0.0123(5)	0.0183(5)	−0.0033(4)	0.0117(4)	−0.0037(4)
S3	0.0159(4)	0.0142(5)	0.0193(5)	−0.0023(4)	0.0138(4)	−0.0020(5)

Note. The expression of the general temperature factor is $\exp(-2\pi(U_{11}h^2a^{*2} + U_{22}k^2b^{*2} + U_{33}l^2c^{*2} + 2U_{12}hka^*b^* + 2U_{13}hla^*c^* + 2U_{23}klb^*c^*)$.

derives from an *ABC* closed packing of sulfur anions. The succession of sulfur layers encloses, in every other gap, triangularly ordered Mn^{II} cations, P_2 pairs, and Ag_2 groups. The particularity of the structure lies in the location of the silver (I) cations (see Fig. 1): Instead of tetrahedral surroundings, as in $Ag_4P_2S_7$, $Ag_4P_2S_6$, or $Ag_7P_3S_{11}$ (*16*) for instance, or octahedral sites, as in the $Ag^IM^{III}P_2P_6$ derivatives (*10*), the Ag(I) ions prefer, in their majority, the center of triangular sulfur faces on the edge of the layers (Ag1 on Fig. 1). Such a localization induces strong distortions on the sulfur net that, in return, shape the Mn and P_2 environment. Very large thermal parameters are found for all silver partially filled positions (see Table IV).

V. Structure Description and Discussion

The location of the Ag1 cations in two opposite triangular faces of the sulfur octahedra leads to an Ag1–Ag1 separation of 338 pm. In the (AgS_3) group, the calculated Ag1-to-sulfur distances (246.9, 247.1, and 248.1 pm) fit well in between the classical Ag^I–S distances for two collinear bonds (241 pm) and those for tetrahedral bonds (262 pm) (*17*). In addition, they match the Ag–S distances of other planar 3-coordination geometry, for instance that observed in Ag_3AsS_3 (251 pm) (*18*) and in $AgSbS_2$ (251 pm) (*19*). The sulfur triangles the large Ag^I cations occupy are considerably enlarged (d_{S-S} = 428 pm) in comparison with those of $Mn_2P_2S_6$ (mean d_{S-S} = 357 pm). Such an

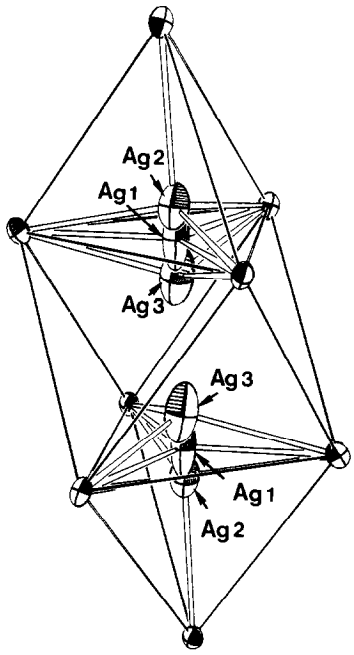

FIG. 1. ORTEP view of Ag^I site distribution in $Ag_2MnP_2S_6$ (Ag1: 81%, Ag2: 13%, and Ag3: 8%).

expansion reacts upon the other triangles: If the S_3 equilateral units surrounding P_2 pairs almost do not change (d_{S-S} = 337 pm versus d_{S-S} = 339 pm in MnP_2S_6), the P–S bonds and the S–P–S angles of the PS_3 units strongly oppose any contraction as already observed in $CuVP_2S_6$ (*12b*). The S_3 groups sandwiching the Mn^{II} cations narrow down (d_{S-S} = 341 pm versus d_{S-S} = 357 pm in MnP_2S_6). This narrowing generates a major distortion within the Mn^{II} octahedra. Indeed, the S–Mn–S angles drift far beyond regular 90 and 180° angles (see Table V). However, the Mn–S distances remain homogeneous and, moreover, almost correspond to that of $Mn_2P_2S_6$ (d_{Mn-S} = 260 pm versus d_{Mn-S} = 262 pm in MnP_2S_6). This cannot occur without a widening of the slab (measured between sulfur plans at the anions centers, from 325 pm in MnP_2S_6 to 341 pm) stretching out the P–P bond (from 218.7 pm in MnP_2S_6 to 223.4 pm), in accord with the flexibility of this one in the P_2S_6 units known to be flexible (they range from 214.8 pm in $Ni_2P_2S_6$ to 222.2 pm in $Cd_2P_2S_6$). Therefore, the calculated Ag1–Ag1 distance (338 pm) is in rather direct relation with the slab thickness (341 pm). For manganese (II) cations, it happens that the M^{II}–S bonds adapt themselves to the widening of the slab through S–Mn–S angle distortions. The d^{10} silver cations are thus not structurally forced to short homoatomic contact; then they do not interact. This structural pattern would require a much smaller M^{II} cation to constrain the Ag^I to a relative proximity and then authorize d^{10}–d^{10} interactions; with their small ionic radii, Ni^{II} or Mg^{II}, for instance, might be good candidates to test that assumption.

Another consequence of the large expansion of the triangles that hold the Ag^I cations is a twisting of the Mn^{II} and P_2 sulfur octahedra toward a prismatic geometry (18° about the axis perpendicular to the slabs, see Fig. 2). That distortion shortens one half of the S–S through-the-slab contacts. Nevertheless, those contacts remain well above the van der Waals limit ($d_{S-S\ min}$ = 368 pm $\gg d_{vdW}$ = 305 pm); they do not contribute to the slab widening and should not go against a slab thickness reduction in the attempt of a small M^{II} cation substitution.

In our split model description of $Ag_2MnP_2S_6$ structure, on each side of the preponderant Ag1 atom (81% of the whole silver content) stand two sites of minor contribution (Ag2: 13% and Ag3: 8%). All silver atoms present high thermal parameters in the direction perpendicular to the slab ($U_{33} > 0.05 \times 10^4$ pm^2, see Table IV). With a single crystal X-ray analysis, the genuine nature of the disorder (static or dynamic) cannot be determined. If two Ag1 and Ag3 silver atoms simultaneously occupy their site, they would be closer than in metallic silver (277 pm versus 289 pm) and could show some sort of d^{10}–d^{10} interaction. Such a situation cannot be ruled out but is felt un-

TABLE V

MAIN INTERATOMIC ANGLES (°) AND DISTANCES (pm) IN $Ag_2MnP_2S_6$

P–S1 : 203.0(1)	
P–S2 : 203.9(1)	P–P : 223.4(2)
P–S3 : 202.9(1)	
($P–S_{avg}$: 203.3)	
Mn–S1 (×2) : 258.73(9)	S1–Mn–S1 : 91.05(4)
Mn–S2 (×2) : 264.68(8)	S1–Mn–S2 (×2) : 109.51(3)
Mn–S3 (×2) : 257.92(9)	S1–Mn–S2 (×2) : 81.09(2)
	S1–Mn–S3 (×2) : 166.13(3)
($Mn–S_{avg}$: 260.4)	S1–Mn–S3 (×2) : 82.41(2)
	S2–Mn–S2 : 165.32(4)
	S2–Mn–S3 (×2) : 81.65(3)
	S2–Mn–S3 (×2) : 89.56(3)
	S3–Mn–S3 : 106.47(4)
Ag1–S1 : 246.9(2)	S1–Ag1–S2 : 120.11(7)
Ag1–S2 : 248.1(2)	S1–Ag1–S3 : 120.70(7)
Ag1–S3 : 247.1(2)	S2–Ag1–S3 : 119.17(8)
Ag2–S1 : 259(1)	S1–Ag2–S2 : 115.1(5)
Ag2–S2 : 249(1)	S1–Ag2–S3 : 116.4(5)
Ag2–S3 : 246(1)	S2–Ag2–S3 : 119.2(4)
Ag2–S2 : 275(1)	S1–Ag2–S2 : 94.5(3)
	S2–Ag2–S2 : 106.2(5)
	S2–Ag2–S3 : 99.9(5)
Ag3–S1 : 240(2)	Ag1–Ag1 : 338(3) through the slab
Ag3–S2 : 267(2)	Ag1–Ag3 : 277(5) through the slab
Ag3–S3 : 260(2)	Ag2–Ag2 : 315(3) through the gap

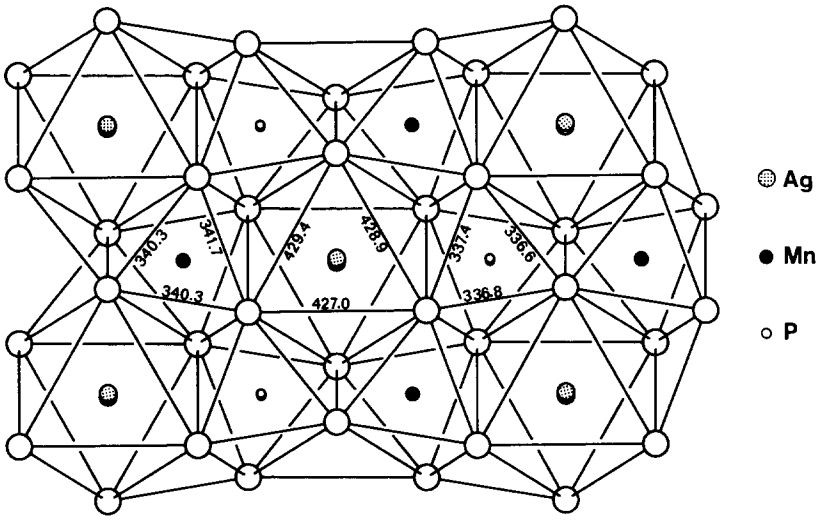

FIG. 2. Triangular cationic arrangement in the two-dimensional sheet of $Ag_2MnP_2S_6$ phase. The sulfur to sulfur distances of the sheet triangles are lengthened for Ag(I) site, maintained for P_2 site, and shrunk for Mn sites.

likely. The Ag2 atoms, displaced toward the tetrahedral sites in the van der Waals gap, offer two sets of distances with the sulfur anion ligands (e.g., three short ones 246, 249, and 259 pm and a long one 275 pm). In addition, of the three silver positions, it is the one with the smallest thermal parameters. This is to relate to similar features reported for copper positions in $CuVP_2S_6$ (*12b*). Two Ag2 atoms that would set simultaneously into two adjacent in-gap tetrahedra would be closer to each other than the Ag1 atoms are through the slab (315 pm versus 338 pm). Despite the presence of some silver cations in the gap, there is not much broadening of the interlayer space with regard to that of $Mn_2P_2S_6$ (319 pm versus 323 pm).

The point to be emphasized, in the $Ag_2MnP_2S_6$ structure, is the simultaneous occurrence of Ag^+ cations into two (AgS_3) triangles of the slab octahedra. From the only interslab silver to silver distance, and taking into account the van der Waals radius of that element, it is unlikely that any homobond exists. If one considers the strong distortions and the mutual repulsion involved, he or she may wonder why Ag^+ cations concurrently occupy these two sites. In effect, it should be pointed at that this does not seem to be the only solution within the chosen framework; a structure with, for instance, Ag^+ in an octahedral site within the slab and another one in a tetrahedral or octahedral site within the gap can be imagined.

The above exposed results totally confirm the assumptions, on the overall $Ag_2MnP_2S_6$ arrangement, as found from IR and Raman spectroscopy observations (*14*). For instance, the perturbation of the P_2S_6 units (with regard to that of the $Mn_2P_2S_6$ phase), the ordered distribution of the P_2S_6, $M^{II}S_6$, and $(Ag^I)_2S_6$ entities on the intralamellar sites, and the large vibrational amplitudes of the silver ions proved correct. Furthermore, the occupation by silver ions of an interslab site, as deduced from conductivity measurements (*20*) (carried out from 300 K up), may correspond to the

observed in-gap Ag2 site. A striking point, nevertheless, is the departure of the EXAFS findings (*13*) from those of the present study: If the triangular environment of silver cations was clearly deduced from EXAFS spectra fittings, the calculated Ag–S distances (234(3) pm for the first sulfur neighbors) largely contrast with that of our single crystal least-squares results ($d_{Ag-S\ min}$ = 246.9(2) pm). So far, no explanations that could elucidate the difference have been found. It is noteworthy to point out that the same discrepancy was observed for $CuCrP_2S_6$ between EXAFS and diffraction results (*21*).

VI. Magnetic Properties

Sintered samples were selected for magnetic susceptibility measurements that were carried on a Faraday balance apparatus in the 4.2–300 K temperature range. The variation versus temperature, of the reciprocal molar magnetic susceptibility ($1/\chi$ mole) (corrected for diamagnetic contribution), is presented in Fig. 3. Above 40 K, a linear variation is observed, that is, χ^{-1} obeys the Curie–Weiss law $1/\chi$ mole = $(T - \theta_p)/C_{mole}$, where θ_p and C_{mole} are the Weiss constant and the molar Curie constant, respectively. The latter constant C_{mole} = 58.0 × 10^{-6} $m^3.K.mole^{-1}$, least-squares refined from the data in the range 40–300 K, is very close to the calculated spin-only molar Curie constant of Mn^{II} cations (54.9 × 10^{-6} $m^3.K.mole^{-1}$); it thus confirms our charge assignment $(Ag^{1+})_2(Mn^{2+})(P_2S_6)^{4-}$. The former constant, θ_p = −42.5 K, indicates preponderant interactions of the antiferromagnetic type. At lower temperature, the molar susceptibility increases rapidly within a range of few degrees just above the transition temperature T_N that is estimated to be around 9 K. This is indicative of a possible Dzialoshinski effect (*22*), corresponding to an antiferromagnetism in which both magnetic nets are misaligned. A nonsymmetric coupling between the spins, that can be inferred from the silver distribution, may be responsible for that misalignment.

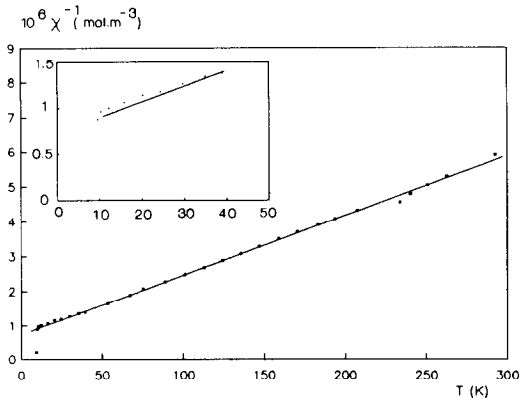

FIG. 3. Reciprocal molar magnetic susceptibility (corrected for core magnetism) vs temperature of $Ag_2MnP_2S_6$ in the range 4.2–300 K.

VII. Conclusion

The structure determination of $Ag_2MnP_2S_6$ helped to reveal the Ag^+ behavior in that phase and confirmed the simultaneous presence of two silver per octahedron. The occurrence of Ag–Ag homobonds could be ruled out, whereas the rather usual feature of coinage elements was found (i.e., high thermal coefficients in multiple coordination symmetries). One of the factors assumed to be responsible for this arrangement is the high stability of silver (I) trigonal coordination since other types of coordination are possible within the structure. New frameworks based upon more ionic species should help study the influence of local potentials with regard to the type of coordination exerted by d^{10} elements, whereas studies of structural changes as a function of temperature should shed some light on their true local mobility.

Acknowledgment

The authors especially thank T. Massil for the preliminary studies carried out on $Ag_2MnP_2S_6$ crystals.

References

1. M. JANSEN, *Angew. Chem. Int. Ed. Engl.* **26,** 1098 (1987).
2. A. F. WELLS, "Structural Inorganic Chemistry," 4th ed., Oxford Univ. Press (Clarendon), London/New York (1975).
3. C. FRIEBEL AND M. JANSEN, *Z. Natürforsch. B* **39,** 739 (1984).
4. D. B. ROGERS, R. D. SHANNON, J. PREWITT, AND J. L. CILLSON, *Inorg. Chem.* **10,** 723 (1971).
5. P. K. MEHROTRA AND R. HOFFMANN, *Inorg. Chem.* **17,** 2187 (1978).
6. Y. JIANG, S. ALVAREZ, AND R. HOFFMANN, *Inorg. Chem.* **24,** 749 (1985).
7. L. E. ORGEL, *J. Chem. Soc.* 4186 (1958).
8. (a) G. OUVARD, R. BREC, AND J. ROUXEL, *Mater. Res. Bull.* **20,** 1181 (1985); (b) E. PROUZET, G. OUVARD, AND R. BREC, *Mater. Res. Bull.* **21,** 643 (1986).
9. M. BARJ, G. LUCAZEAU, G. OUVARD, AND R. BREC, *Eur. J. Solid State Inorg. Chem.* **25,** 449 (1988).
10. (a) P. COLOMBET, A. LEBLANC, M. DANOT, AND J. ROUXEL, *Nouv. J. Chim.* **7,** 333 (1983); (b) S. LEE, P. COLOMBET, G. OUVRARD, AND R. BREC, *Mater. Res. Bull.* **21,** 917 (1986).
11. G. OUVRARD AND R. BREC, *Mater. Res. Bull.* **23,** 1199 (1988).
12. (a) P. COLOMBET, A. LEBLANC, M. DANOT, AND J. ROUXEL, *J. Solid State Chem.* **41,** 174 (1982); (b) E. DURAND, G. OUVRARD, M. EVAIN, AND R. BREC, *Inorg. Chem.*, submitted for publication (1990).
13. Z. LI AND Y. MATHEY, *J. Chim. Phys.* **86,** 1665 (1989).
14. (a) Y. MATHEY, R. CLEMENT, J. P. AUDIERE, O. POIZAT, AND C. SOURISSEAU, *Solid State Ionics* **9, 10,** 459 (1983); (b) O. POIZAT AND C. SOURISSEAU, *J. Solid State Chem.* **59,** 371 (1985); (c) O. POIZAT, C. SOURISSEAU, AND Y. MATHEY, *J. Solid State Chem.* **72,** 272 (1988); (d) O. POIZAT, F. FILLAUX, AND C. SOURISSEAU, *J. Solid State Chem.* **72,** 283 (1988).
15. B. FRENZ, "Enraf–Nonius, Structure Determination Package," Delft Univ. Press (1982).
16. (a) P. TOFFOLI, P. KHODADAD, AND N. RODIER, *Acta Crystallogr., Sect. B* **33,** 1492 (1977); (b) P. TOFFOLI, A. MICHELET, P. KHODADAD, AND N. RODIER, *Acta Crystallogr., Sect., B* **38,** 706 (1982); (c) P. TOFFOLI, P. KHODADAD, AND N. RODIER, *Acta Crystallogr., Sect. B* **38,** 2374 (1982).
17. R. D. SHANNON, "Structure and Bonding in Crystals" (M. O'Keeffe and A. Navrotsky, Eds.), Vol. 2, p. 61, Academic Press, San Diego (1981).
18. VON P. ENGEL AND W. NOWACKI, *Acta Crystallogr., Sect. B* **24,** 77 (1968).
19. C. R. KNOWLES, *Acta Crystallogr.* **17,** 847 (1964).
20. O. POIZAT, Y. MATHEY, AND C. SOURISSEAU, "Galerne," France (1984).
21. Y. MATHEY, A. MICHALOWICZ, P. TOFFOLI, AND G. VLAIC, *Inorg. Chem.* **23,** 897 (1984).
22. I. DZIALOSHINSKI, *Phys. Chem. Solids* **4,** 241 (1958).